



Measurement-Device-Independent Quantum Key Distribution over 200 km

Yan-Lin Tang,^{1,2} Hua-Lei Yin,^{1,2} Si-Jing Chen,³ Yang Liu,^{1,2} Wei-Jun Zhang,³ Xiao Jiang,^{1,2†} Lu Zhang,³ Jian Wang,^{1,2} Li-Xing You,³ Jian-Yu Guan,^{1,2} Dong-Xu Yang,^{1,2} Zhen Wang,³ Hao Liang,^{1,2} Zhen Zhang,^{4,2} Nan Zhou,^{1,2} Xiongfeng Ma,^{4,2‡} Teng-Yun Chen,^{1,2§} Qiang Zhang,^{1,2*} and Jian-Wei Pan^{1,2}

¹National Laboratory for Physical Sciences at Microscale and Department of Modern Physics, Shanghai Branch, University of Science and Technology of China, Hefei, Anhui 230026, China

²CAS Center for Excellence and Synergetic Innovation Center in Quantum Information and Quantum Physics, Shanghai Branch, University of Science and Technology of China, Hefei, Anhui 230026, China

³State Key Laboratory of Functional Materials for Informatics, Shanghai Institute of Microsystem and Information Technology, Chinese Academy of Sciences, Shanghai 200050, China

⁴Center for Quantum Information, Institute for Interdisciplinary Information Sciences, Tsinghua University, Beijing 100084, China

(Received 30 July 2014; published 6 November 2014)

Measurement-device-independent quantum key distribution (MDIQKD) protocol is immune to all attacks on detection and guarantees the information-theoretical security even with imperfect single-photon detectors. Recently, several proof-of-principle demonstrations of MDIQKD have been achieved. Those experiments, although novel, are implemented through limited distance with a key rate less than 0.1 bit/s. Here, by developing a 75 MHz clock rate fully automatic and highly stable system and superconducting nanowire single-photon detectors with detection efficiencies of more than 40%, we extend the secure transmission distance of MDIQKD to 200 km and achieve a secure key rate 3 orders of magnitude higher. These results pave the way towards a quantum network with measurement-device-independent security.

DOI: 10.1103/PhysRevLett.113.190501

PACS numbers: 03.67.Dd, 03.67.Ac, 03.67.Hk

Quantum key distribution (QKD) [1,2] offers the most appealing solution for secure key exchange by providing information-theoretical security. Despite tremendous experimental developments, practical QKD systems still suffer from various attacks rooted in their deviations from the theoretical models in security proofs. The security of the measurement-device-independent quantum key distribution (MDIQKD) protocol [3], inspired by the time-reversed EPR-based QKD protocol [4,5], does not rely on any assumption on measurement. Compared with the regular QKD system where Eve can take advantage of the side information of the detection devices, the MDIQKD protocol allows Eve to have full control of the measurement devices without any key information leakage. Thus, it is naturally immune to all detection attacks [6–10], which are believed to be the main threat to practical QKD systems. Meanwhile, the MDIQKD protocol not only provides security with imperfect detectors but also is able to achieve performance comparable to the regular prepare-and-measure QKD systems [11–14].

Because of its security and practicability, the MDIQKD protocol has attracted extensive attention in the field. Until now, many efforts have been devoted to experimental demonstrations of the MDIQKD protocol using time-bin phase-encoding schemes [15,16] and polarization-encoding schemes [17,18]. Previously, two full implementations of the MDIQKD protocol, which employed the decoy-state method [19–21] to guarantee the security of source, achieved the secure key rates of 0.12 [16] and 0.0047 bit/s [18] over

50 and 10 km fiber links, respectively. These experimental demonstrations have formed a solid basis for the feasibility of MDIQKD systems. However, compared with standard QKD systems, these demonstrations have limited transmission distances and low key rates. The demonstration of the practicability of the MDIQKD protocol is still missing.

In this Letter, by improving the system clock rate, single-photon detector efficiency, and stability, we achieve the secure transmission distance of 200 km and improve the secure key rate by 3 orders of magnitude compared to that of previous demonstrations.

The MDIQKD experiment setup is illustrated in Fig. 1(a), where one can see that the positions of Alice and Bob are symmetric. Alice's (Bob's) signal laser source (1550 nm) is internally modulated into a pulse train with a width of 2.5 ns and a clock rate of 75 MHz, compared with 1 MHz in previous experiments [15–18]. The directly modulated pulse trains' phases are intrinsically random to make sure the system is immune to the unambiguous-state-discrimination attack [22]. Alice (Bob) uses an amplitude modulator (AM) to randomly modulate the laser into three different intensities according to the decoy-state method, one as signal state intensity ($\mu = 0.4$), another as decoy-state intensity ($\nu = 0.07$), and the rest as the vacuum-state intensity (0). Their probability distributions are set as 33%, 45%, and 22%. The setting of the intensity and probability distributions is optimized at the distance of 200 km and is adopted for all the distances in our experiment.

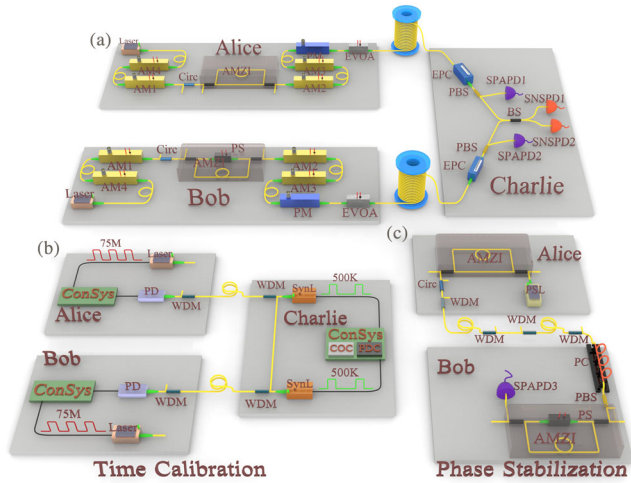


FIG. 1 (color online). (a) Schematic layout of our MDIQKD setup. Alice's (Bob's) signal laser pulses (1550 nm) are modulated into three decoy-state intensities by AM1. An AMZI, an AM2–4, and one PM are used to encode qubits. Charlie's setup consists of a polarization stabilization system and a BSM system. The polarization stabilization system in each link includes an EPC, a PBS, and a SPAPD. The BSM system includes an interference BS and two SNSPDs. (b) Time calibration system. Two SynLs (1570 nm) are adopted, with the 500 kHz shared time reference generated from a crystal oscillator circuit (COC) and with the time delayed by a programmable delay chip (PDC). Alice (Bob) receives the SynL pulses with a PD and then regenerates a system clock of 75 MHz. WDM: wavelength division multiplexer, ConSys: control system. (c) Phase stabilization system. Circ: circulator, PC: polarization controller, PS: phase shifter.

We employ the time-bin phase-encoding scheme and utilize a combination of an asymmetrical Mach-Zehnder interferometer (AMZI), three AMs, and one phase modulator (PM) to encode qubits. The AMZI divides the laser pulse into two time bins separated by a 6.5 ns time delay. For the Z basis, the key bit is encoded in time bin, 0 or 1, by AM2 and AM3. For the X basis, the key bit is encoded into the relative phase, 0 or π , by PM. AM4 is used to normalize the average photon numbers in the Z basis and X basis. All the modulators, including the AMs and the PM, are controlled by the random numbers of Alice and Bob independently. We remark that in order to increase the fidelity of time bin 0 or 1, we exploit two AMs for the Z-basis encoding. Beneficially, this arrangement helps to improve the extinction ratio of the vacuum state in the decoy-state method. An electrical variable optical attenuator has two functionalities: the first is to set the signal laser pulses to single-photon level in QKD procedure; the second is to set the intensity of signal laser pulses to be strong enough in time calibration procedure for the time calibration system to accumulate enough signal count to measure the averaged arriving time of signal laser pulses precisely.

The laser pulses of Alice (Bob) go through an SMF-28 fiber spool of the length ranging from 25 to 100 km in each

arm, to interfere with the ones sent by Bob (Alice). In the middle, Charlie takes a partial Bell state measurement (BSM). The critical challenge for our system is to develop a stable BSM system for two independent laser pulses traveling through two 100-km-fiber links, under a high clock rate. Note that it is not a trivial upgrade compared with the previous MDIQKD systems, because under a high clock rate, the task imposes a technical challenge on laser modulation, rigorous timing, and frequency calibration. Furthermore, the time and polarization drifting due to the 200 km channel adds even more challenge to the experiment.

In our setup, we optimize the laser waveform and the scheme of vacuum-state generation for high-clock-rate laser modulation (detailed in Sec. III of the Supplemental Material [23]). Additionally, we develop several automatic feedback systems to calibrate the time, spectrum, and polarization modes of the two independent laser pulses.

For the timing mode shown in Fig. 1(b), two synchronization laser (SynL, 1570 nm) pulse trains are sent through two additional fiber links from Charlie to Alice and Bob, with shared time references generated by a crystal oscillator circuit at Charlie's site. Alice (Bob) utilizes a photoelectric detector (PD) to detect the SynL pulses. The output signals of the PD are used to regenerate a 75 MHz system clock so that the whole system can be synchronized. Then we precisely overlap the two signal laser pulse trains via a feedback control. Alice and Bob alternatively send the signal laser pulses to Charlie. Charlie uses the superconducting nanowire single-photon detector (SNSPD) to measure the arriving time of the signal laser pulses. On the basis of the arriving time difference, Charlie adjusts the time delay between the two SynL pulse trains with a programmable delay chip. The timing resolution is 10 ps and the total timing calibration precision is below 20 ps, both of which are much smaller than the 2.5 ns pulse width of the signal laser.

For the spectrum mode, we utilize an optical spectrum analyzer (OSA) and a temperature-controlled circuit built in the laser to acquire and then compensate the central wavelength difference of Alice's and Bob's lasers. We first select two nearly identical laser diodes as Alice's and Bob's laser sources, considering the aspects of both the same full width at half maximum (FWHM) wavelength and the same central wavelength. Then we utilize this OSA to measure the difference between the two central wavelengths of Alice's and Bob's lasers with a precision of 1 pm. This precision is decided by the sampling interval and repeatability of the OSA [29] if the relative wavelength difference of two lasers is more important than the precise wavelength value in some scenario. At last, we set the two laser wavelengths as the same by adjusting their temperatures through the temperature-controlled circuits built in the lasers. The controlling precision of the central wavelength is about 0.5 pm. Then the difference between Alice's and Bob's spectrum modes can be controlled to be smaller than

the spectrum span of the laser pulses, in our case, 4 pm (FWHM) measured by the Fabry-Perot interference method with a resolution of 0.06 pm.

For the polarization mode, we adopt a polarization stabilization system comprised of an electric polarization controller (EPC), a polarization beam splitter (PBS), and an InGaAs/InP single-photon avalanche photodiode (SPAPD). We insert the EPC and PBS before the interference beam splitter (BS) and connect the transmission port of PBS with the BS. The reflection port of the PBS is monitored by the SPAPD, whose count rate is used as the feedback signal to control the EPC. With the use of this polarization stabilization system operated in real time, the polarization mode is maintained and the fluctuation of received laser power in Charlie's site is controlled to be less than 3%.

Besides these calibration systems above, we adopt a phase stabilization system [16] to maintain the phase reference frames of Alice's and Bob's phase-encoding setups, as shown in Fig. 1(c). The phase reference frame, namely, the relative phase between AMZI's two arms, may fluctuate with temperature and stress, and the fluctuation will introduce further errors in the X basis. To stabilize this, we employ a pulsed phase-stabilization laser (PSL, 1550 nm) with a pulse width of 2.5 ns. Alice sends the laser pulses of PSL through Alice's and Bob's AMZIs connected by an additional fiber between Alice and Bob. Bob monitors the power at an output of his AMZI with another InGaAs/InP SPAPD. The phase is then calibrated by a phase shifter inside Bob's AMZI. Additionally, we put the AMZIs in a thermal container to isolate the temperature and stress perturbation.

All the aforementioned feedback systems contribute to a good interference and high stabilization, and the automatic calibration procedure can largely improve the time utilization efficiency. While the previous experiment [16] needs to manually calibrate the interference per 15 min, the current setup can remain working for more than 1 day.

In Charlie's site, a partial BSM is implemented with an interference BS and two SNSPDs. The insertion loss of the measurement system is 1 dB. A Bell state is postselected when the two detectors in the two output arms of the BS have a coincidence at two alternative time bins; i.e., the first detector has an event at time bin 0 (1) and simultaneously the second detector has an event at time bin 1 (0). Since the key is generated based on two detectors' coincidence measurements, MDIQKD has a higher requirement for the detector efficiency compared with that of the regular QKD scheme. In the experiment, we develop a multichannel SNSPD system cooled by a Gifford-McMahon cryocooler. The SNSPDs are fabricated from ultrathin NbN film on SiO₂/Si substrate with a typical meandered nanowire structure and an optical cavity structure. No bandpass filter is included [30]. Operated at 2.2 K, two SNSPDs provide the system detection efficiencies of 46% and 40% at the dark count rate of 10 Hz, respectively, which are almost 2 or 3

times higher than the efficiency in previous experiments. In order to achieve a better signal to noise ratio, we adopt a time window of 1.5 ns, 60% of the pulse width of 2.5 ns.

After Charlie announces the BSM results, Alice and Bob then sift out a raw key stream and generate the final secure key through error correction and privacy amplification, detailed in Sec. I of the Supplemental Material [23]. We assume that the secure key is extracted from the data when both Alice and Bob encode their pulses using signal states in the Z basis. The secure key rate formula is [3,20]

$$R \geq Q_{11}^{\mu\mu}[1 - H(e_{11}^{\mu\mu})] - Q^{\mu\mu}fH(E^{\mu\mu}), \quad (1)$$

where $Q^{\mu\mu}$ and $E^{\mu\mu}$ are the overall gain and error rate when both sources generate signal states. $Q_{11}^{\mu\mu}$ and $e_{11}^{\mu\mu}$, the gain and phase error rate when both sources generate single-photon states within signal states, can be estimated by the decoy-state method. The parameter f is the error correction efficiency, and we take the value $f = 1.16$ in our calculation. $H(e) = -e\log_2(e) - (1 - e)\log_2(1 - e)$ is the binary Shannon entropy function.

We have continuously run the system in the laboratory for 130 h with spooled fibers of distances of 50, 100, 150, and 200 km. The details for the experimental results can be found in Sec. II of the Supplemental Material [23]. To calculate the secure key rate, we use the decoy-state method [31] to estimate $Q_{11}^{\mu\mu}$ and $e_{11}^{\mu\mu}$ and make the finite-key analysis with the Chernoff bound [32], which is preferred to provide better and stricter parameter estimation in the high-loss situation in long-distance QKD. We adopt a tight failure probability of 2×10^{-9} , which is 6 orders of magnitude lower than the previous ones [16,18]. This is detailed in Sec. I of the Supplemental Material [23]. As shown in Fig. 2, the secure key rates are marked, which fit the theoretical curve well. We note that the key rates are information-theoretically secure with a failure probability of 2×10^{-9} , which are the lower bounds for key generation required by the security proof. Previous experimental results [16,18] are also shown in Fig. 2 for comparison. One can see that we have improved the secure key rate by 3 orders of magnitude compared with the previous results [16,18].

Taking for example the experiment result of the 200 km detailed in the Supplemental Material [23], we can see that $E^{\mu\nu}$ ($\mu, \nu \neq 0$) of the Z basis is less than 0.25%, owing to the fact that the two AMs employed to encode the Z -basis qubits contribute to an extinction ratio of more than 40 dB. Meanwhile, $E^{\mu\mu}$ of the X basis is less than 26% compared with the typical value of 25%, from which we can infer that the interference of Alice's and Bob's laser pulse is good and the automatic feedback systems operate effectively. Through error correction and privacy amplification, the secure key length obtained is 8.31 kbits and the secure key rate is 0.018 bit/s.

With this MDIQKD system, we have extended the distribution distance from 50 to 200 km and filled the

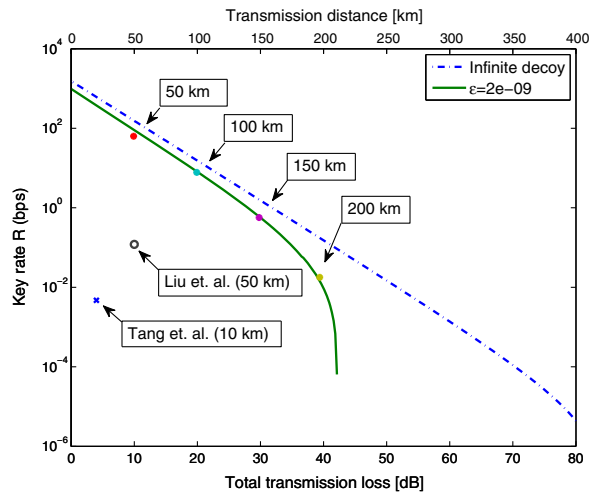


FIG. 2 (color online). Secure key rates of experiments in the laboratory as well as the simulation results. The four dots correspond to the experimental results with the fiber transmitting loss of 9.9 dB (50 km), 19.9 dB (100 km), 29.8 dB (150 km), and 39.6 dB (200 km). The solid curve shows the result calculated by simulating the vacuum + weak decoy-state scheme with the experimental parameters. The dashed curve represents the optimal result with infinite number of decoy states.

gap of attainable distance between the MDIQKD protocol and the regular Bennett-Brassard 1984 protocol. In addition, with an optimized decoy-state scheme, the secure key rate is higher than the previous results by 3 orders of magnitude. Furthermore, we adopt the Chernoff bound to make a better and stricter statistical fluctuation analysis. The failure probability of 2×10^{-9} is 6 orders of magnitude lower than the previous ones [16,18]. These results have moved MDIQKD towards a more practical setting. To demonstrate the feasibility of MDIQKD in an unstable environment, we have moved the system into an installed fiber network and implemented a field test [33].

We remark that the techniques developed in our MDIQKD system constitute a critical ingredient for a quantum repeater [34] and pave the way for long-distance quantum communication. The time calibration and automatic feedback system we developed demonstrates that the interference of two independent lasers over 200 km is feasible and stable. Besides, the MDIQKD protocol has an intrinsic property that is desirable for constructing a quantum network [35] with the star-type structure, since the detection system placed in the BSM site (as a server) can be shared by all the transmitters. To add more transmitters in the network, we only need the laser sources and the modulators, which are much cheaper and smaller than the detection system. We expect that the MDIQKD network can be built within reach of current technology and become mature in the near future.

We remark that we provide several techniques for the optimization of high-speed laser modulation, which is of great importance for further improvement of system clock

rate. With a better overall timing jitter, we can expect GHz clock rate with the state-of-the-art components [11]. There is still much room for the further improvement of SNSPD efficiency [36]. We can extrapolate that the transmission distance and secure key rate can be further improved by increasing the clock rate and detector efficiency. Furthermore, in our experiment, we use two different fibers to transmit signal laser pulses and synchronization laser pulses, respectively. In order to increase the appeal of MDIQKD in real-world applications, it would be desirable to use a single fiber to transmit both the signal laser pulses and the synchronization laser pulses [37] and minimize the noise generated from Raman spontaneous scattering [38]. This remains an important work for real-world applications in the future.

The authors would like to thank X. Xie, M. Jiang, and Q. Mao for enlightening discussions and C. Luo especially for her experimental assistance. This work was supported by the National Fundamental Research Program (under Grants No. 2011CB921300, No. 2013CB336800, and No. 2011CBA00300), the National Natural Science Foundation of China, the Chinese Academy of Science, and the Shandong Institute of Quantum Science & Technology Co., Ltd.

*Corresponding author.

qiangzh@ustc.edu.cn

†jiangx@ustc.edu.cn

‡xiongfengma@gmail.com

§tychen@ustc.edu.cn

- [1] C. H. Bennett and G. Brassard, in *Proceedings of IEEE International Conference on Computers, Systems, and Signal Processing* (IEEE, New York, Bangalore, India, 1984), pp. 175–179.
- [2] A. K. Ekert, *Phys. Rev. Lett.* **67**, 661 (1991).
- [3] H.-K. Lo, M. Curty, and B. Qi, *Phys. Rev. Lett.* **108**, 130503 (2012).
- [4] E. Biham, B. Huttner, and T. Mor, *Phys. Rev. A* **54**, 2651 (1996).
- [5] H. Inamori, *Algorithmica* **34**, 340 (2002).
- [6] V. Makarov, A. Anisimov, and J. Skaar, *Phys. Rev. A* **74**, 022313 (2006).
- [7] B. Qi, C.-H. F. Fung, H.-K. Lo, and X. Ma, *Quantum Inf. Comput.* **7**, 073 (2007).
- [8] L. Lydersen, C. Wiechers, C. Wittmann, D. Elser, J. Skaar, and V. Makarov, *Nat. Photonics* **4**, 686 (2010).
- [9] H. Weier, H. Krauss, M. Rau, M. Fürst, S. Nauerth, and H. Weinfurter, *New J. Phys.* **13**, 073024 (2011).
- [10] A. N. Bugge, S. Sauge, A. M. M. Ghazali, J. Skaar, L. Lydersen, and V. Makarov, *Phys. Rev. Lett.* **112**, 070503 (2014).
- [11] H. Takesue, S. W. Nam, Q. Zhang, R. H. Hadfield, T. Honjo, K. Tamaki, and Y. Yamamoto, *Nat. Photonics* **1**, 343 (2007).
- [12] Y. Liu, T.-Y. Chen, J. Wang, W.-Q. Cai, X. Wan, L.-K. Chen, J.-H. Wang, S.-B. Liu, H. Liang, L. Yang *et al.*, *Opt. Express* **18**, 8587 (2010).

- [13] D. Stucki, N. Walenta, F. Vannel, R. T. Thew, N. Gisin, H. Zbinden, S. Gray, C. Towery, and S. Ten, *New J. Phys.* **11**, 075003 (2009).
- [14] S. Wang, W. Chen, J.-F. Guo, Z.-Q. Yin, H.-W. Li, Z. Zhou, G.-C. Guo, and Z.-F. Han, *Opt. Lett.* **37**, 1008 (2012).
- [15] A. Rubenok, J. A. Slater, P. Chan, I. Lucio-Martinez, and W. Tittel, *Phys. Rev. Lett.* **111**, 130501 (2013).
- [16] Y. Liu, T.-Y. Chen, L.-J. Wang, H. Liang, G.-L. Shentu, J. Wang, K. Cui, H.-L. Yin, N.-L. Liu, L. Li *et al.*, *Phys. Rev. Lett.* **111**, 130502 (2013).
- [17] T. Ferreira da Silva, D. Vitoreti, G. B. Xavier, G. C. do Amaral, G. P. Temporão, and J. P. von der Weid, *Phys. Rev. A* **88**, 052303 (2013).
- [18] Z. Tang, Z. Liao, F. Xu, B. Qi, L. Qian, and H.-K. Lo, *Phys. Rev. Lett.* **112**, 190503 (2014).
- [19] W.-Y. Hwang, *Phys. Rev. Lett.* **91**, 057901 (2003).
- [20] H.-K. Lo, X. Ma, and K. Chen, *Phys. Rev. Lett.* **94**, 230504 (2005).
- [21] X.-B. Wang, *Phys. Rev. Lett.* **94**, 230503 (2005).
- [22] Y.-L. Tang, H.-L. Yin, X. Ma, C.-H. F. Fung, Y. Liu, H.-L. Yong, T.-Y. Chen, C.-Z. Peng, Z.-B. Chen, and J.-W. Pan, *Phys. Rev. A* **88**, 022308 (2013).
- [23] See Supplemental Material at <http://link.aps.org/supplemental/10.1103/PhysRevLett.113.190501>, which includes Refs. [24–28].
- [24] D. Gottesman, H.-K. Lo, N. Lütkenhaus, and J. Preskill, *Quantum Inf. Comput.* **4**, 325 (2004).
- [25] C.-H. F. Fung, X. Ma, and H. F. Chau, *Phys. Rev. A* **81**, 012318 (2010).
- [26] M. Koashi and J. Preskill, *Phys. Rev. Lett.* **90**, 057902 (2003).
- [27] H. Chernoff, *Ann. Math. Stat.* **23**, 493 (1952).
- [28] X. Ma, C.-H. F. Fung, and M. Razavi, *Phys. Rev. A* **86**, 052305 (2012).
- [29] http://support.us.yokogawa.com/downloads/TMI/COMM/AQ6370B/IM735302-01E_010.pdf.
- [30] X.-Y. Yang, H. Li, W.-J. Zhang, L.-X. You, X.-Y. Liu, Z. Wang, W. Peng, X.-M. Xie, and M.-H. Jiang, *Opt. Express* **22**, 16267 (2014).
- [31] F. Xu, M. Curty, B. Qi, and H.-K. Lo, *New J. Phys.* **15**, 113007 (2013).
- [32] M. Curty, F. Xu, W. Cui, C. C. W. Lim, K. Tamaki, and H.-K. Lo, *Nat. Commun.* **5**, 3732 (2014).
- [33] Y.-L. Tang, H.-L. Yin, S.-J. Chen, Y. Liu, W.-J. Zhang, X. Jiang, L. Zhang, J. Wang, L.-X. You, J.-Y. Guan *et al.*, [arXiv:1408.2330](https://arxiv.org/abs/1408.2330).
- [34] H.-J. Briegel, W. Dür, J. I. Cirac, and P. Zoller, *Phys. Rev. Lett.* **81**, 5932 (1998).
- [35] J. Qiu, *Nature (London)* **508**, 441 (2014).
- [36] F. Marsili, V. Verma, J. Stern, S. Harrington, A. Lita, T. Gerrits, I. Vayshenker, B. Baek, M. Shaw, R. Mirin *et al.*, *Nat. Photonics* **7**, 210 (2013).
- [37] T. E. Chapuran, P. Toliver, N. A. Peters, J. Jackel, M. S. Goodman, R. J. Runser, S. R. McNow, N. Dallmann, R. J. Hughes, K. P. McCabe *et al.*, *New J. Phys.* **11**, 105001 (2009); G. B. Xavier and J. P. Von der Weid, *Electron. Lett.* **46**, 1071 (2010); I. Choi, R. J. Young, and P. D. Townsend, *Opt. Express* **18**, 9600 (2010); K. A. Patel, J. F. Dynes, I. Choi, A. W. Sharpe, A. R. Dixon, Z. L. Yuan, R. V. Penty, and A. J. Shields, *Phys. Rev. X* **2**, 041010 (2012).
- [38] D. Subacius, A. Zavriyev, and A. Trifonov, *Appl. Phys. Lett.* **86**, 011103 (2005); T. Ferreira da Silva, G. Xavier, G. Temporao, and J. von der Weid, *J. Lightwave Technol.* **32**, 2332 (2014).